Applied Mathematics Letters 104 (2020) 106226

Contents lists available at ScienceDirect

Applied Mathematics Letters

www.elsevier.com/locate/aml

# A domain-decomposition generalized finite difference method for stress analysis in three-dimensional composite materials

Yuanyuan Wang [a], Yan Gu [a,*], Jianlin Liu [b]

[a] School of Mathematics and Statistics, Qingdao University, Qingdao 266071, PR China
[b] Department of Engineering Mechanics, College of Pipeline and Civil Engineering, China University of Petroleum (East China), Qingdao 266580, PR China

ARTICLE INFO

*Article history:*
Received 31 December 2019
Received in revised form 10 January 2020
Accepted 11 January 2020
Available online 17 January 2020

*Keywords:*
Meshless method
Generalized finite difference method
Domain decomposition technique
Stress analysis
Composite materials

ABSTRACT

In this paper, a new framework for stress analysis of three-dimensional (3D) composite (multi-layered) elastic materials is presented. In our computations, the composite material is firstly decomposed into several sub-domains by using the domain-decomposition technique, and then in each of the sub-domain, the stresses are approximated by using a meshless generalized finite difference method (GFDM). Along the sub-domain interfaces, compatibility of displacements and equilibrium of tractions are imposed. The new method yields a sparse and banded matrix system which makes it very attractive for large-scale engineering simulations. Numerical examples with up to 500,000 unknowns are solved successfully using the developed GFDM code.



## 1. Introduction

The generalized finite difference method (GFDM) has emerged as a robust meshless method for various engineering applications [1–4]. The method uses the Taylor series expansions and the moving least squares approximation to derive explicit formulae for the required partial derivatives of unknown variables. The method is truly meshless and can be applied for solving problems merely defined over irregular clouds of points. The advantages of the method, as compared with the standard finite element (FEM) and boundary element (BEM) methods [5,6], are thoroughly discussed in Refs. [7,8]. All these attractive features with the GFDM have attracted continued interests from scientific researchers.

In this study, we document the first attempt to extend the frontiers of the GFDM, in conjunction with a domain-decomposition technique, to stress analysis of three-dimensional (3D) multi-layered elastic materials. The proposed domain-decomposition GFDM (DD-GFDM) scheme has been proposed to combine the advantages of the domain-decomposition technique and the high accuracy of the GFDM to yield a

* Corresponding author.
*E-mail address:* guyan1913@163.com (Y. Gu).

https://doi.org/10.1016/j.aml.2020.106226

new framework that is suitable for large-scale engineering simulations. In our computations, the whole computational domain is firstly decomposed into several sub-domains along the interfaces of the composite material, and then in each of the sub-domain, the displacement and stress solutions are approximated by using the standard GFDM formulation. By enforcing the satisfaction of the displacement and traction compatibility conditions along the interfaces, a system of sparse and banded system matrices can be formed. The new method can now solve large-scale problems [9] with up to 500,000 unknowns on a desktop computer without any difficulty.

## 2. Statement of the basic problem

The governing equations for 3D elasticity problem, also known as the Navier equation, with respect to the displacements $u_1(\boldsymbol{x})$, $u_2(\boldsymbol{x})$ and $u_3(\boldsymbol{x})$, can be expressed as [10]:

$$\left\{2\frac{1-\mu}{1-2\mu}\right\}\frac{\partial^2 u_1(\boldsymbol{x})}{\partial x^2}+\frac{\partial^2 u_1(\boldsymbol{x})}{\partial y^2}+\frac{\partial^2 u_1(\boldsymbol{x})}{\partial z^2}+\left\{\frac{1}{1-2\mu}\right\}\frac{\partial^2 u_2(\boldsymbol{x})}{\partial x\partial y}+\left\{\frac{1}{1-2\mu}\right\}\frac{\partial^2 u_3(\boldsymbol{x})}{\partial x\partial z}=f_1(\boldsymbol{x}), \quad (1)$$

$$\left\{\frac{1}{1-2\mu}\right\}\frac{\partial^2 u_1(\boldsymbol{x})}{\partial x\partial y}+\frac{\partial^2 u_2(\boldsymbol{x})}{\partial x^2}+\left\{2\frac{1-\mu}{1-2\mu}\right\}\frac{\partial^2 u_2(\boldsymbol{x})}{\partial y^2}+\frac{\partial^2 u_2(\boldsymbol{x})}{\partial z^2}+\left\{\frac{1}{1-2\mu}\right\}\frac{\partial^2 u_3(\boldsymbol{x})}{\partial y\partial z}=f_2(\boldsymbol{x}), \quad (2)$$

$$\left\{\frac{1}{1-2\mu}\right\}\frac{\partial^2 u_1(\boldsymbol{x})}{\partial x\partial z}+\left\{\frac{1}{1-2\mu}\right\}\frac{\partial^2 u_2(\boldsymbol{x})}{\partial y\partial z}+\frac{\partial^2 u_3(\boldsymbol{x})}{\partial x^2}+\frac{\partial^2 u_3(\boldsymbol{x})}{\partial y^2}+\left\{2\frac{1-\mu}{1-2\mu}\right\}\frac{\partial^2 u_3(\boldsymbol{x})}{\partial z^2}=f_3(\boldsymbol{x}), \quad (3)$$

where $\boldsymbol{x}=(x,y,z)$, $\mu$ is the Poison's ratio, $f_i(\boldsymbol{x})$, $i=1,2,3$ are the known inhomogeneous terms. The strains $\varepsilon_{ij}(\boldsymbol{x})$, $i,j=1,2,3$, are related to displacements by the following relations:

$$\varepsilon_{ij}(\boldsymbol{x})=[\partial u_i(\boldsymbol{x})/\partial x_j+\partial u_j(\boldsymbol{x})/\partial x_i]/2, \quad (4)$$

and the stresses $\sigma_{ij}(\boldsymbol{x})$ are related to strains through Hooke's low by:

$$\sigma_{ij}(\boldsymbol{x})=2G[\varepsilon_{ij}(\boldsymbol{x})+\mu\varepsilon_{kk}(\boldsymbol{x})\delta_{ij}/(1-2\mu)], \quad (5)$$

where $G$ is the shear modulus and $\delta_{ij}$ denotes the Kronecker delta. Here and in the following, the customary Einstein's notation for summation over repeated subscripts is employed. According to elasticity theory, the boundary tractions $t_i(\boldsymbol{x})$, $i=1,2,3$, are defined in terms of stresses as:

$$t_i(\boldsymbol{x})=\sigma_{ij}(\boldsymbol{x})n_j(\boldsymbol{x}), \quad \boldsymbol{x}\in\Gamma, \quad (6)$$

where $n_j(\boldsymbol{x})$ is the direction cosine of the unit outward normal vector at the boundary point $\boldsymbol{x}$. Eqs. (1)–(6) completely describe the elastic boundary-value problem.

## 3. Generalized finite difference method (GFDM) and its numerical implementation

In the GFDM approach, a cloud of nodes is discretized inside the whole computational domain $\Omega$. Every node inside $\Omega$ should be regarded as a central node $\boldsymbol{x}_0$. The $m$ nearest supporting nodes $\boldsymbol{x}_i$, $i=1,\ldots,m$ around $\boldsymbol{x}_0$ should be found. The concept of the 'local subdomain' then refers to the small area containing $\boldsymbol{x}_0$ and $\boldsymbol{x}_i$ . Without loss of generality, let us consider the following general differential equation in a 3D domain:

$$a_1\frac{\partial U}{\partial x}+a_2\frac{\partial U}{\partial y}+a_3\frac{\partial U}{\partial z}+a_4\frac{\partial^2 U}{\partial x^2}+a_5\frac{\partial^2 U}{\partial y^2}+a_6\frac{\partial^2 U}{\partial z^2}+a_7\frac{\partial^2 U}{\partial x\partial y}+a_8\frac{\partial^2 U}{\partial x\partial z}+a_9\frac{\partial^2 U}{\partial y\partial z}=f(\boldsymbol{x}), \quad (7)$$

where the coefficients $a_i$, $i=1,2,\ldots,9$, are constants. Suppose $U_0$ is the function value at point $\boldsymbol{x}_0$ and $U_i$, $i=1,\ldots,m$ the function values at points $\boldsymbol{x}_i$, $i=1,\ldots,m$, then $U_i$ can be expanded at point $\boldsymbol{x}_0$ by using the following Taylor series expansion:

$$U_i=U_0+h_i\frac{\partial U_0}{\partial x}+k_i\frac{\partial U_0}{\partial y}+l_i\frac{\partial U_0}{\partial z}+\frac{1}{2}\left(h_i^2\frac{\partial^2 U_0}{\partial x^2}+k_i^2\frac{\partial^2 U_0}{\partial y^2}+l_i^2\frac{\partial^2 U_0}{\partial z^2}\right)+\cdots, \quad i=1,2,\ldots,m, \quad (8)$$

where $(h_i, k_i, l_i) = (x_i - x_0, y_i - y_0, z_i - z_0)$ with the notations $\boldsymbol{x}_i = (x_i, y_i, z_i)$ and $\boldsymbol{x}_0 = (x_0, y_0, z_0)$. We can define the following error function by omitting the second-order derivatives in Eq. (8)

$$B(U) = \sum_{i=1}^{m} \left[ \left( U_0 - U_i + h_i \frac{\partial U_0}{\partial x} + k_i \frac{\partial U_0}{\partial y} + \cdots + h_i l_i \frac{\partial^2 U_0}{\partial x \partial z} + k_i l_i \frac{\partial^2 U_0}{\partial y \partial z} \right) \omega_i(h_i, k_i, l_i) \right]^2, \tag{9}$$

where $\omega_i(h_i, k_i, l_i)$ is the weighting function (quartic-spline), as defined in Ref. [11]. Let us define:

$$\boldsymbol{D}_U = \left\{ \frac{\partial U_0}{\partial x}, \frac{\partial U_0}{\partial y}, \frac{\partial U_0}{\partial z}, \frac{\partial^2 U_0}{\partial x^2}, \frac{\partial^2 U_0}{\partial y^2}, \frac{\partial^2 U_0}{\partial z^2}, \frac{\partial^2 U_0}{\partial x \partial y}, \frac{\partial^2 U_0}{\partial x \partial z}, \frac{\partial^2 U_0}{\partial y \partial z} \right\}, \tag{10}$$

and minimize $B(U)$ with respect to $\boldsymbol{D}_U$, one has:

$$\partial B(U) / \partial \{\boldsymbol{D}_U\} = 0. \tag{11}$$

On solving Eq. (11), we can obtain the following linear equation system:

$$\boldsymbol{A}\boldsymbol{D}_U = \boldsymbol{b}, \tag{12}$$

and the vector $\boldsymbol{D}_U$ can now be expressed as

$$\boldsymbol{D}_U = \boldsymbol{A}^{-1}\boldsymbol{b}. \tag{13}$$

Now we can observe from Eq. (13) that the partial derivatives $\boldsymbol{D}_U$ at point $\boldsymbol{x}_0$ have been expressed by combinations of variable values at its neighboring points inside the local subdomain. It is interesting to note that the GFDM matrix $\boldsymbol{A}$ is positive definite with a unique Cholesky decomposition, and therefore, the condition number of $\boldsymbol{A}$ is relatively moderate. Substituting Eq. (13) into the governing Eq. (7) could yield a linear algebraic equation. The final GFDM results can then be calculated on solving this matrix system. We refer interested readers for Refs. [7,12] for further details. It is interesting to note that the concept of star in the GFDM yields a sparse matrix system in contrast to a fully populated matrix in, for example, the MFS and BEM. Therefore, the GFDM is very efficient to analyze problems defined in high dimensions and complex geometries.

## 4. Non-overlapping domain-decomposition GFDM (DD-GFDM)

A generic 3D layered material is illustrated in Fig. 1(a), where the entire domain is decomposed into two sub-domains $\Omega^{\mathrm{I}}$ and $\Omega^{\mathrm{II}}$. The exterior boundary of sub-domain $\Omega^{\mathrm{I}}$ is $\Gamma^{\mathrm{I}}$ and that of sub-domain $\Omega^{\mathrm{II}}$ is $\Gamma^{\mathrm{II}}$. The interface between the two sub-domains is denoted by $\Gamma^{\mathrm{c}}$. The Poison's ratio and shear modulus associated with $\Omega^{\mathrm{I}}$ and $\Omega^{\mathrm{II}}$ are represented by $\mu^{\mathrm{I}}, \mu^{\mathrm{II}}$ and $G^{\mathrm{I}}, G^{\mathrm{II}}$, respectively. In the DD-GFDM approach, we treat the two sub-domains $\Omega^{\mathrm{I}}$ and $\Omega^{\mathrm{II}}$ separately. In sub-domain $\Omega^{\mathrm{I}}$, the following discretized algebraic equations can be obtained:

$$[F^{\mathrm{I}}] \begin{pmatrix} \{u^{\mathrm{I}}\} \\ \{u_c^{\mathrm{I}}\} \end{pmatrix} = \{U^{\mathrm{I}}\} \ , \ [F_c^{\mathrm{I}}] \begin{pmatrix} \{u^{\mathrm{I}}\} \\ \{u_c^{\mathrm{I}}\} \end{pmatrix} = \{U_c^{\mathrm{I}}\}, \ [H^{\mathrm{I}}] \begin{pmatrix} \{u^{\mathrm{I}}\} \\ \{u_c^{\mathrm{I}}\} \end{pmatrix} = \{T^{\mathrm{I}}\} \ , \ [H_c^{\mathrm{I}}] \begin{pmatrix} \{u^{\mathrm{I}}\} \\ \{u_c^{\mathrm{I}}\} \end{pmatrix} = \{T_c^{\mathrm{I}}\}, \tag{14}$$

where $U_c^{\mathrm{I}}, T_c^{\mathrm{I}}$ and $u_c^{\mathrm{I}}$ denote the interface displacements, tractions, and the unknown variables of sub-domain $\Omega^{\mathrm{I}}$ on the interface $\Gamma_c, U^{\mathrm{I}}, T^{\mathrm{I}}$ and $u^{\mathrm{I}}$ the displacements, tractions, and the unknown variables of sub-domain $\Omega^{\mathrm{I}}$ on the remaining surfaces. $F^{\mathrm{I}}, F_c^{\mathrm{I}}, H^{\mathrm{I}}$, and $H_c^{\mathrm{I}}$ are coefficient matrices of the GFDM expansion. Similarly, for the sub-domain $\Omega^{\mathrm{II}}$, we have:

$$[F^{\mathrm{II}}] \begin{pmatrix} \{u^{\mathrm{II}}\} \\ \{u_c^{\mathrm{II}}\} \end{pmatrix} = \{U^{\mathrm{II}}\} \ , \ [F_c^{\mathrm{II}}] \begin{pmatrix} \{u^{\mathrm{II}}\} \\ \{u_c^{\mathrm{II}}\} \end{pmatrix} = \{U_c^{\mathrm{II}}\}, \ [H^{\mathrm{II}}] \begin{pmatrix} \{u^{\mathrm{II}}\} \\ \{u_c^{\mathrm{II}}\} \end{pmatrix} = \{T^{\mathrm{II}}\} \ , \ [H_c^{\mathrm{II}}] \begin{pmatrix} \{u^{\mathrm{II}}\} \\ \{u_c^{\mathrm{II}}\} \end{pmatrix} = \{T_c^{\mathrm{II}}\}. \tag{15}$$

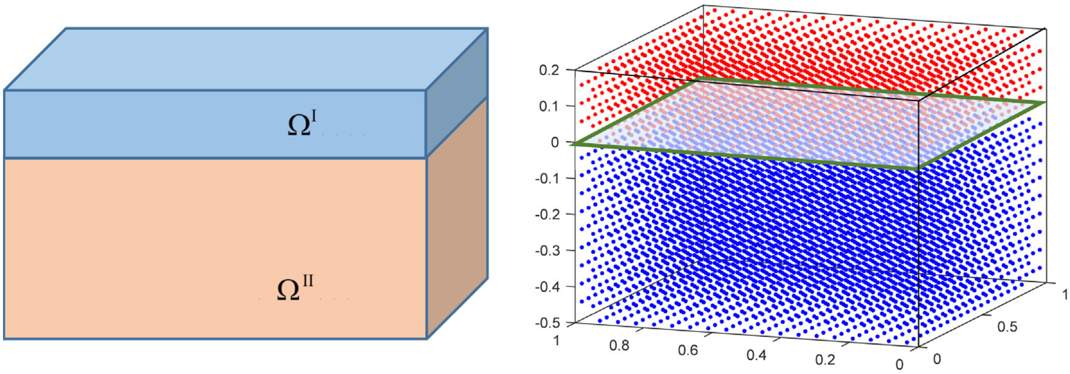


(a) Geometry of the problem (b) Nodes distribution of the DD-GFDM model

**Fig. 1.** Geometry of the problem (a) and the nodes distribution of the DD-GFDM model.

To solve the problem numerically, there will be the same number of algebraic equations as the unknowns. Therefore, the following continuity conditions at the interface must be considered:

$$T_{cn} = T_{cn}^{\mathrm{I}} = -T_{cn}^{\mathrm{II}},\ T_{ct} = T_{ct}^{\mathrm{I}} = -T_{ct}^{\mathrm{II}}, \tag{16}$$

$$U_{cn} = U_{cn}^{\mathrm{I}} = U_{cn}^{\mathrm{II}},\ U_{ct} = U_{ct}^{\mathrm{I}} = U_{ct}^{\mathrm{II}}, \tag{17}$$

where the subscript $(cn)$ indicates interface $\Gamma_c$ and normal $(n)$ component, and subscript $(ct)$ stands for interface $\Gamma_c$ and tangential $(t)$ direction. We here suppose that the traction boundary conditions are prescribed on the external surfaces of $\Gamma_{\mathrm{I}}$, and displacement boundary conditions are prescribed on the external surfaces of $\Gamma_{\mathrm{II}}$. According to the equilibrium and compatibility conditions (16) and (17) at the interface, Eqs. (14)–(15) can be coupled as:

$$\begin{pmatrix} [H^{\mathrm{I}}] & [0] \\ [F_c^{\mathrm{I}}] & -[F_c^{\mathrm{II}}] \\ [H_c^{\mathrm{I}}] & [H_c^{\mathrm{II}}] \\ [0] & [F^{\mathrm{II}}] \end{pmatrix} \begin{bmatrix} \begin{pmatrix} \{u^{\mathrm{I}}\} \\ \{u_c^{\mathrm{I}}\} \end{pmatrix} \\ \begin{pmatrix} \{u^{\mathrm{II}}\} \\ \{u_c^{\mathrm{II}}\} \end{pmatrix} \end{bmatrix} = \begin{bmatrix} \{T^{\mathrm{I}}\} \\ \{0\} \\ \{0\} \\ \{U^{\mathrm{II}}\} \end{bmatrix}, \tag{18}$$

More equations will be added to this system in a similar way for other layers and the substrate. The system still needs to be reordered according to the prescribed boundary conditions.

## 5. Numerical results and discussions

To verify the methodologies developed above, one benchmark numerical examples are examined in which the proposed DD-GFDM solutions are compared with the corresponding exact solutions. The relative error defined below is employed [13,14]:

$$Relative\ Error = \left[\sum_{i=1}^{M} [I_{\mathrm{numer}}(i) - I_{exact}(i)]^2\right]^{1/2} \Bigg/ \left[\sum_{i=1}^{M} [I_{exact}(i)]^2\right]^{1/2}, \tag{19}$$

where $I_{\mathrm{numerical}}$ and $I_{exact}$ denote the numerical and analytical results, respectively. In this example, we consider a composite material where we take $\Omega^{\mathrm{I}}$ to be a cubic $(0,1) \times (0,1) \times (0,0.2)$ and $\Omega^{\mathrm{II}}$ to be $(0,1) \times (0,1) \times (-0.5,0)$, as shown in Fig. 1(b). The elastic constants are $\mu^{\mathrm{I}} = 0.3$, $G^{\mathrm{I}} = 5 \times 10^6$ for

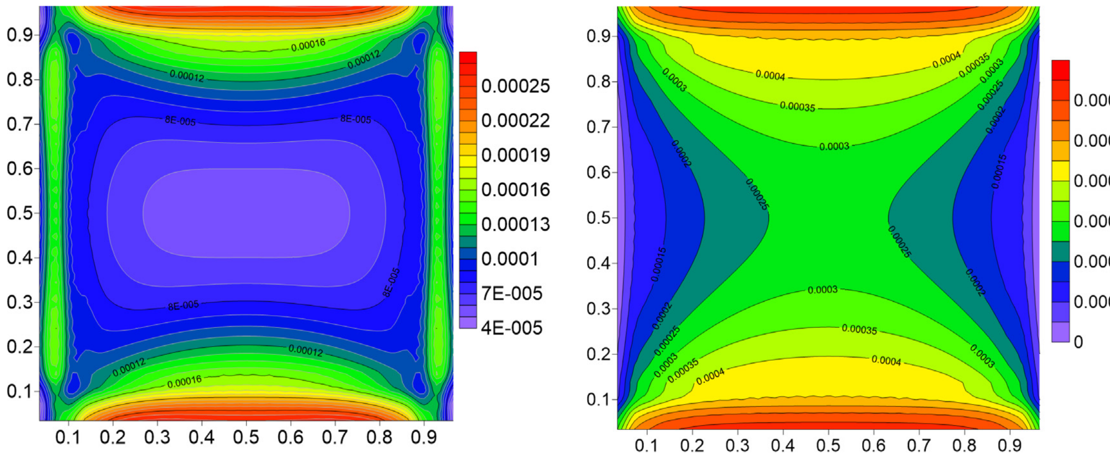


(a) Relative errors of stresses

(b) Relative errors of stresses

**Fig. 2.** Relative errors of the calculated stresses at points along the interface of the material.

$\Omega^{\mathrm{I}}$, and $\mu^{\mathrm{II}} = 0.1$, $G^{\mathrm{II}} = 4 \times 10^6$ for $\Omega^{\mathrm{II}}$. For the ease of comparison, we considered the following analytical solutions:

$$u_1(\boldsymbol{x}) = \frac{(1-\mu)}{2(1+\mu)G} xz^2, \;\; u_2(\boldsymbol{x}) = \frac{(1-\mu)}{2(1+\mu)G} yz^2, \;\; u_3(\boldsymbol{x}) = \frac{1}{4(1+\mu)G} z^2, \tag{20}$$

where $\mu = \mu^{\mathrm{I}}$ and $G = G^{\mathrm{I}}$ for $\Omega^{\mathrm{I}}$, and $\mu = \mu^{\mathrm{II}}$ and $G = G^{\mathrm{II}}$ for $\Omega^{\mathrm{II}}$. This 3D model is subjected to a mixed-type boundary conditions, where the tractions are prescribed on the external surfaces of domain $\Omega^{\mathrm{I}}$ and displacements are prescribed on the external surfaces of $\Omega^{\mathrm{II}}$.

For the numerical implementation, a total number of 20,160 GFDM nodes are discretized inside the whole computational domain. Fig. 2 shows the contours of relative errors of the calculated stresses $\sigma_{11}$ and $\sigma_{22}$ at the interface of the composite material. It can be seen that the stresses predicted by the proposed DD-GFDM are in excellent agreement with their corresponding analytical solutions. It is also observed that the DD-GFDM results with only 20,160 nodes are quite accurate for this layered material, and the size of the resulting system of linear algebraic equations is quite small. In fact, for an i5-2.90 GHz computer, the total CPU times taken to solve this problem are 3.96 CPU seconds for the proposed DD-GFDM model.

In Fig. 3, we illustrate how the global error decays as an increasing number of GFDM nodes. It can be seen that the proposed DD-GFDM model is stable, accurate, and rapidly convergent as the number of GFDM nodes increases. It can be also observed that for the largest model with 500,000 GFDM nodes, the proposed method used only about 81.64 CPU seconds, which makes the method possible for large-scale engineering simulations.

## 6. Concluding remarks

This paper makes the first attempt to apply the generalized finite difference method (GFDM) for stress analysis of 3D elastic composite materials. The multi-layered materials under consideration are solved using a domain-decomposition technique, in which the whole computational domain is decomposed into several sub-domains and, in each of the sub-domain, the displacement and stress solutions are approximated by using the GFDM simulations. Our preliminary numerical experiment shows that the proposed domain-decomposition GFDM is very promising for accurate and efficient numerical simulations of multi-layered materials. The method also offers great promise in the analysis of many other problems, including flow/convection problems, wave propagations, non-linear and advection–diffusion problems. Some work along these lines is already underway and will be reported in the subsequent papers.

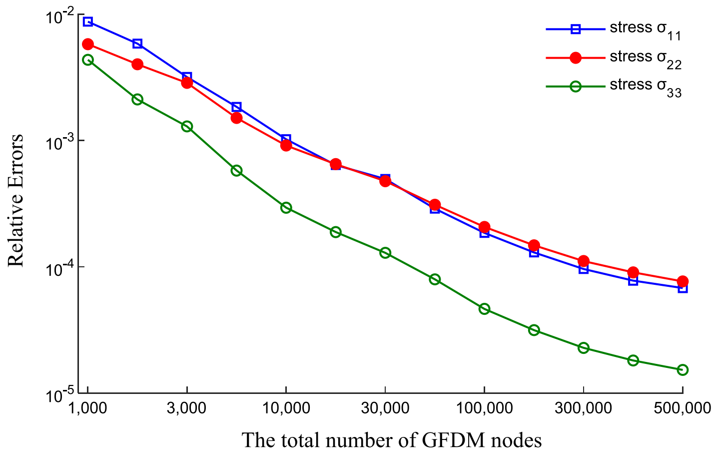


**Fig. 3.** Relative error curves of calculated stresses inside the whole domain.

## CRediT authorship contribution statement

**Yuanyuan Wang:** Writing - original draft. **Yan Gu:** Conceptualization, Methodology. **Jianlin Liu:** Visualization, Investigation.

## Acknowledgments

The work described in this paper was supported by the National Natural Science Foundation of China (No. 11872220), and the Natural Science Foundation of Shandong Province of China (ZR2017BA003, ZR2015GZ007, ZR2017JL004).

## References

[1] J.J. Benito, F. Urena, L. Gavete, Solving parabolic and hyperbolic equations by the generalized finite difference method, J. Comput. Appl. Math. 209 (2) (2007) 208–233.
[2] C.M. Fan, Y.K. Huang, P.W. Li, C.L. Chiu, Application of the generlized finite-difference method to inverse biharmonic boundary-value problems, Numer. Heat Transfer B 65 (2) (2014) 129–154.
[3] W. Qu, A high accuracy method for long-time evolution of acoustic wave equation, Appl. Math. Lett. 98 (2019) 135–141.
[4] Y. Gu, H. Sun, A meshless method for solving three-dimensional time fractional diffusion equation with variable-order derivatives, Appl. Math. Model. 78 (2020) 539–549.
[5] C. Cheng, Z. Niu, H. Zhou, N. Recho, Evaluation of multiple stress singularity orders of a V-notch by the boundary element method, Eng. Anal. Bound. Elem. 33 (10) (2009) 1145–1151.
[6] Z.-J. Fu, Q. Xi, W. Chen, A.H.D. Cheng, A boundary-type meshless solver for transient heat conduction analysis of slender functionally graded materials with exponential variations, Comput. Math. Appl. 76 (4) (2018) 760–773.
[7] Y. Gu, W. Qu, W. Chen, L. Song, C. Zhang, The generalized finite difference method for long-time dynamic modeling of three-dimensional coupled thermoelasticity problems, J. Comput. Phys. 384 (2019) 42–59.
[8] S. Chen, W. Wang, X. Zhao, An interpolating element-free Galerkin scaled boundary method applied to structural dynamic analysis, Appl. Math. Model. 75 (2019) 494–505.
[9] J. Xiao, W. Ye, Y. Cai, J. Zhang, Precorrected FFT accelerated BEM for large-scale transient elastodynamic analysis using frequency-domain approach, Internat. J. Numer. Methods Engrg. 90 (1) (2012) 116–134.
[10] Q.G. Liu, B. Šarler, Non-singular method of fundamental solutions for elasticity problems in three-dimensions, Eng. Anal. Bound. Elem. 96 (2018) 23–35.
[11] Y. Gu, Q. Hua, C. Zhang, X. He, The generalized finite difference method for long-time transient heat conduction in 3D anisotropic composite materials, Appl. Math. Model. 71 (2019) 316–330.
[12] P.-W. Li, C.-M. Fan, Generalized finite difference method for two-dimensional shallow water equations, Eng. Anal. Bound. Elem. 80 (2017) 58–71.
[13] F. Wang, C.-M. Fan, Q. Hua, Y. Gu, Localized MFS for the inverse Cauchy problems of two-dimensional Laplace and biharmonic equations, Appl. Math. Comput. 364 (2020) 124658.
[14] W. Qu, Y. Gu, Y. Zhang, C.-M. Fan, C. Zhang, A combined scheme of generalized finite difference method and Krylov deferred correction technique for highly accurate solution of transient heat conduction problems, Internat. J. Numer. Methods Engrg. 117 (1) (2019) 63–83.